Proceedings of the 2001 IEEE
International Conference on Robotics & Automation
Seoul, Korea · May 21-26, 2001

A visual servoing algorithm based on epipolar geometry

G. Chesi, D. Prattichizzo, A. Vicino

Dipartimento di Ingegneria dell'Informazione - Università di Siena
Via Roma, 56 - 53100 Siena, Italy
email: {chesi,prattichizzo,vicino}@dii.unisi.it

Abstract

A visual servoing algorithm for mobile robots is proposed. The main feature of the algorithm is that it exploits object profiles rather than solving correspondence problems using object features or texture. This property is crucial for mobile robot navigation in unstructured environments where the 3D scene exhibits only surfaces whose main features are their apparent contours. The framework is based on the epipolar geometry, which is recovered from object profiles and epipolar tangencies. Special symmetry conditions of epipoles are used to generate the mobile robot control law. For the sake of simplicity, mobile robot kinematics is assumed to be holonomic and the camera intrinsic parameters are assumed partially known. Such assumption can be relaxed to extend the application field of the approach.

1 Introduction

This paper deals with the problem of controlling the pose of a mobile robot with respect to a target object by means of visual feedback.

Visual servoing has been applied recently to mobile robotics, see e.g. [6, 8, 4]. In visual servoing, the control goals and the feedback law are directly designed in the image domain. Designing the feedback at the sensor level increases system performance especially when uncertainties and disturbances can affect the robot model and the camera calibration [7].

In [7] the authors presented a classification of visual servoing systems. The approach used in this paper is known as image-based visual servoing, where the error between the robot pose and a target object or a set of target features is computed directly from image features.

Visual servoing algorithms make use of object cues whose image plane projections are controlled to desired positions through the visual servoing process. Usually, these cues are distinctive textures, like corners, of objects in the 3D scene.

However, it may happen that the 3D scene does not exhibit any appropriate textures but only smooth surfaces whose main features consist of their apparent contours, defined as the projection of the contour generators of objects' surfaces [3]. As pointed out in [10], if the object surface does not have any noticeable texture, the object profile is the only information available to estimate the structure of the surface and the motion of the camera.

The aim of this work is to exploit object profiles to synthesize a visual servoing algorithm. It is worthwhile to notice that, in general, tracking object profiles instead of textures can be performed in a more robust way since solutions of correspondence problems are not required. Exploiting profiles in visual servoing is crucial in outdoor navigation where objects in the scene are highly unstructured (hills, trees, etc.) and solving correspondences is a difficult task which usually gives rise to poor results.

Recent results on using apparent contours and profiles to reconstruct object surfaces and recover camera motion are due to Cipolla and his colleagues, see [3, 1] for example. In [1] visual servoing was based on the estimation of the homography between initial and final viewed profiles but the algorithm worked with planar closed contours and required a correspondence optimization procedure.

2 Visual modeling

Assume that a pinhole camera is fixed to a mobile robot moving on a plane. Let z_c be the optical axis of the camera-robot frame $< c >$. The configuration space of the mobile robot (or of the camera) is $R^2 \times SO(2)$, where $SO(2)$ is the special orthogonal group of 2×2 rotation matrices. Let $(Z_c \ 0 \ X_c)^T$ be the camera center position in the base frame $< b >$, and α_c be the rotation angle of the camera-robot with respect to the z-axis of the base frame (see Fig. 1).

For the sake of simplicity a holonomic mobile robot is

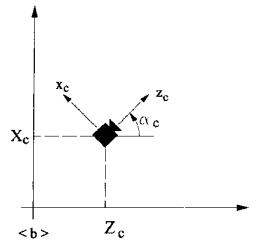

Figure 1: Mobile robot with a fixed camera.

considered. Thus system degrees of freedom are fully actuated by

$$\begin{cases} \dot{Z}_c &= u_z; \\ \dot{X}_c &= u_x; \\ \dot{\alpha}_c &= \omega \end{cases} \tag{1}$$

where $(u_z, u_x)^T$ is the linear velocity of the camera-robot on the plane and ω is the angular velocity about the y-axis.

2.1 Epipolar geometry

Before describing the proposed visual servoing algorithm, we introduce some concepts of epipolar geometry [5, 3]. Consider a pair of cameras with optical centers c', c, optical axes a', a and image planes q', q. The segment $c'c$ is called the *baseline* and its intersections with the image planes define the *epipoles*. The image line passing through the epipole and the image center is called the horizon line, while any plane containing the baseline is called an epipolar plane (see Fig. 2).

Given a pair of views of a scene and a set of corresponding points p'_i, p_i in homogeneous coordinates, there exists a matrix $F \in \mathcal{R}^{3\times3}$, called the *fundamental matrix* [5], such that:

$$p_i'^T F p_i = 0 \ \forall i \tag{2}$$

For any point p_i (p'_i) in one view, the product Fp_i ($F^T p'_i$) defines a line, called the epipolar line, in the other view such that the corresponding point p'_i (p_i) belongs to this line. Moreover, the null right vector of F (F^T) represents the epipole e (e') on the image plane.

Consider now the situation depicted in Fig. 2. Two images are taken by the same camera, which undergoes a rotation θ about the axis o. The optical centers c', c are displaced at the same distance r from the intersection point o of the optical axes. Moreover, image planes and camera rotation axes are perpendicular to the epipolar plane containing o. Under such assumptions and for a camera intrinsic matrix $K = I$, the fundamental matrix

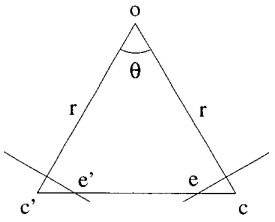

Figure 2: Symmetric camera displacement.

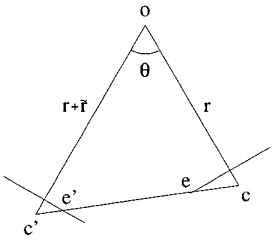

Figure 3: General cameras displacement.

F is given by (see [9, 10] for details):

$$F = \begin{pmatrix} 0 & \cos\theta - 1 & 0 \\ \cos\theta - 1 & 0 & \sin\theta \\ 0 & -\sin\theta & 0 \end{pmatrix} \tag{3}$$

where θ is the angle between the optical axes a' and a, and the epipoles e', e are given by

$$\begin{aligned} e' &= \left(-\tfrac{1}{\tan(\theta/2)},\ 0,\ 1\right)^T, \\ e &= \left(\tfrac{1}{\tan(\theta/2)},\ 0,\ 1\right)^T. \end{aligned} \tag{4}$$

Remark 1 *For the circular displacement in Fig. 2, a special symmetry condition holds: the x-coordinate of the two epipoles in (4) have the same magnitude and opposite sign. Such a symmetry will play a key role in designing the visual servoing algorithm.*

Symmetry is not preserved in the general configuration shown in Fig. 3 where the camera c' is shifted along its optical axis a distance $\tilde{r}$. In this case, the fundamental matrix F assumes the form

$$F = \begin{pmatrix} 0 & \beta\cos\theta - \gamma\sin\theta & 0 \\ -\beta & 0 & \gamma \\ 0 & -\beta\sin\theta - \gamma\cos\theta & 0 \end{pmatrix} \tag{5}$$

where

$$\beta = 1 - \cos\theta - \frac{\tilde{r}}{r + \tilde{r}}, \tag{6}$$

$$\gamma = \sin\theta \tag{7}$$

and the epipoles are $e' = (\alpha',\ 0,\ 1)^T$ and $e = (\alpha,\ 0,\ 1)^T$ with

$$\begin{aligned} \alpha' &= -\left[\tan(\theta/2)\left(1+\tfrac{\tilde{r}}{r}\cdot\tfrac{1}{1-\cos\theta}\right)\right]^{-1}, \\ \alpha &= \left[\tan(\theta/2)\left(1-\tfrac{\tilde{r}}{r+\tilde{r}}\cdot\tfrac{1}{1-\cos\theta}\right)\right]^{-1}. \end{aligned} \tag{8}$$

Remark 2 *The assumption of known camera intrinsic matrix ($K = I$) has been introduced for clarity of presentation. The symmetry property still holds for unknown focal lengths f_x and f_y, and henceforth we will assume that the intrinsic matrix is partially known:*

$$K = \mathrm{diag}(f_x, f_y, 1).$$

Under this assumption, the epipoles are given by

$$\begin{aligned} e' &= (f_x\alpha',\ 0,\ 1)^T \\ e &= (f_x\alpha,\ 0,\ 1)^T \end{aligned} \tag{9}$$

that is, they are obtained by scaling α and α' in (8) by the positive factor f_x.

Finally, note that the camera intrinsic matrix can be assumed completely unknown at the cost of a more involved discussion that, however, would not improve the problem insight.

3 Circular motion

In this section the visual servoing algorithm is described for circular motion. Extensions to general planar motion will be discussed in Section 4.

The core procedure of the proposed visual servoing algorithm consists in exploiting profiles to estimate the epipoles of current and desired images.

Consider the problem of moving a camera from an initial position to a desired position following a circular trajectory on the plane and exploiting only information derived from the desired image and the initial image.

As in Section 2, suppose that the image plane and the rotation axis of the camera are perpendicular to the motion plane, and that the optical axis intersects the trajectory center (see Fig. 2). Two different cases must be analysed.

3.1 Case I: known radius

Assume that the circular trajectory radius r is known. The image of the axis of rotation projects to the vertical line passing through the image center in each view of the scene. According to Section 2.1, the epipoles lie on the horizon line and their position is symmetric with respect to the rotation axis:

$$e' = (-w,\ 0,\ 1)^T; \quad e = (w,\ 0,\ 1)^T$$

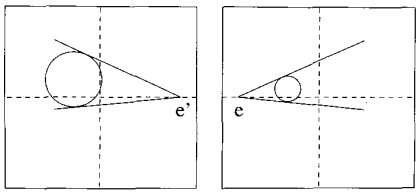

Figure 4: Epipolar tangencies for the symmetric cameras displacement case.

where

$$w = f_x/\tan(\theta/2). \tag{10}$$

This means that the x-coordinates of the epipoles provide informations about the angle θ even when the cameras are uncalibrated.

In what follows, profiles will be exploited to estimate the epipoles of the initial and desired images. The basic idea is to use corresponding profiles in the images in order to estimate the epipole positions. Let *obj* be an object in the scene visible in both views and consider an epipolar plane p (distinct from the horizon plane) tangent to object *obj*. The tangent point between plane p and object *obj* is called *frontier point*: this point has the property of belonging to the apparent contour of object *obj* in each view [3]. Moreover, the epipolar line corresponding to this point is tangent to the apparent contour in each view (see Fig. 4) and, due to the chosen circular motion, the angle between the epipolar tangent and the horizon line is the same in each image.

This suggests that the epipole positions can be found by minimizing the sum of distances between the apparent contour and the corresponding epipolar tangency:

$$w = \underset{\tilde{w}}{\mathrm{argmin}}\left[\mathrm{Dist}(l'(\tilde{w}), C') + \mathrm{Dist}(l(\tilde{w}), C)\right] \tag{11}$$

where $l'(\tilde{w}), l(\tilde{w})$ are the corresponding epipolar lines depending on the epipole positions $\tilde{w}$ and $-\tilde{w}$, C', C are the apparent contours and $Dist(\cdot,\cdot)$ is the distance between the epipolar line and contour. In other words, we are looking for the epipole positions w and $-w$ such that the corresponding epipolar tangent in the current view is an epipolar tangent in the desired view.

Observe that the optimization problem in (11) has only one free parameter w. The visual servoing, leading the robot towards its final position algorithm, is designed on the basis of the estimated parameter w.

Let the circular trajectory of the camera be parameterized as follows (see Fig. 5):

$$\begin{aligned} Z_c(t) &= r\cos\varphi(t), \\ X_c(t) &= r\sin\varphi(t), \\ \alpha_c(t) &= \varphi(t) + \pi \end{aligned} \tag{12}$$

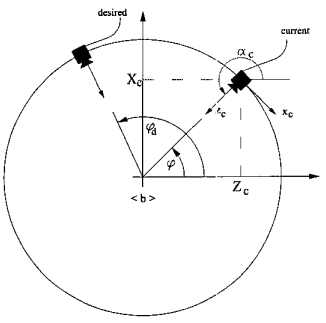

Figure 5: Parameterization of a circular motion centered on the origin of the base frame and with radius r.

where φ is the current camera position angle. The differential kinematics of the system is hence described by:

$$\begin{aligned} \dot{Z}_c(t) &= -X_c(t)\dot{\varphi}(t), \\ \dot{X}_c(t) &= Z_c(t)\dot{\varphi}(t), \\ \dot{\alpha}_c(t) &= \dot{\varphi}(t) \end{aligned} \tag{13}$$

where $\dot{\varphi}(t)$ is the control parameter steering the linear and angular velocity in (1).

To design the visual servoing algorithm, the control parameter $\dot{\varphi}(t)$ must be computable from the image measurement w. Observe that $\theta = \varphi_d - \varphi$, thus when φ approaches the desired value φ_d, $\frac{1}{w}$ decreases and goes to zero for $\varphi = \varphi_d$ as shown in (10), see also Fig. 5.

Therefore, a simple proportional control law of the visual measurement $\frac{1}{w}$ is given by:

$$\dot{\varphi}(t) = \frac{\lambda}{w(t)} \tag{14}$$

for some $\lambda > 0$.

3.2 Case II: unknown radius

Now suppose that the only a priori knowledge of the motion of the camera-robot is that a circular displacement occurs between the desired and the initial positions about an axis perpendicular to the motion plane and passing through an unknown point of the optical axis z_c. The trajectory radius r is unknown.

Let the initial configuration c_i and desired camera position c be as given as shown in Fig. 6. Starting from an initial guess $\hat{r}_0$ for the trajectory radius, apply controls ω, u_z and u_x (angular and linear velocities) as in (13) and (14). If $\hat{r}_0 \neq r$, the camera leaves the circular trajectory of radius r and reaches the new configuration c', after some amount of time, as shown in Fig. 6. The desired image and the current one (that taken by the camera in c') do not exhibit the property of symmetry discussed in Remark 1. In this new configuration (c', c), the epipoles are not symmetric with respect to the rotation axis and their positions are given by (9).

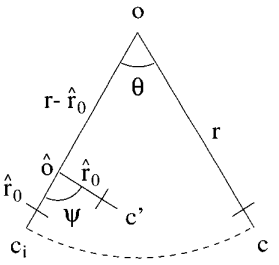

Figure 6: Robot motion under a (circular) control law with a wrong estimate of the radius.

Two parameters, e_u and e_s, can be defined as:

$$e_u = \frac{1}{f_x\alpha'} + \frac{1}{f_x\alpha}, \tag{15}$$

$$e_s = \frac{1}{f_x\alpha'} - \frac{1}{f_x\alpha}. \tag{16}$$

The parameter e_u is defined as the sum of the inverse of the x-coordinates of the two epipoles. It accounts for the unsymmetric part of the displacements between the two views. On the other hand, parameter e_s accounts for the angle θ and as in Section 3.1 will steer the camera along the circular trajectory with known radius.

The following properties hold and are relevant for the design of the visual servoing procedure:

$$e_u\tilde{r} \leq 0, \tag{17}$$

$$e_s(\varphi - \varphi_d) \geq 0. \tag{18}$$

In order to define the visual servoing procedure, we must compute the camera position c', obtained by rotating the camera of the angle ψ about an estimate of the rotation center $\hat{o}$ (Fig. 6).

The general camera position and orientation c' along the (unknown radius) trajectory with respect to the initial position c_i can be written as

$$\begin{aligned} Z_c(t) &= (r - \hat{r}(t))\cos\varphi_i + \hat{r}(t)\cos(\varphi_i + \psi(t)), \\ X_c(t) &= (r - \hat{r}(t))\sin\varphi_i + \hat{r}(t)\sin(\varphi_i + \psi(t)), \\ \alpha_c(t) &= \varphi_i + \psi(t) + \pi \end{aligned} \tag{19}$$

where $\hat{r}(0) = \hat{r}_0$, $\psi(0) = 0$ and φ_i identifies the initial camera position c_i on the plane. Note that the camera orientation at c' is such that the optical axis intersects $\hat{o}$. The corresponding differential kinematics are obtained

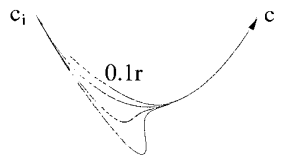

Figure 7: Trajectories followed for different initial estimates $\hat{r}_0$: $0.1r$, r, $2r$ and $3r$ (decreasing order).

by differentiating:

$$\begin{aligned}
\dot{Z}_c(t) &= \dot{\hat{r}}(t)\left[\cos\left(\varphi_i+\psi(t)\right)-\cos\varphi_i\right] \\
&\quad -\hat{r}(t)\dot{\psi}(t)\sin\left(\varphi_i+\psi(t)\right), \\
\dot{X}_c(t) &= \dot{\hat{r}}(t)\left[\sin\left(\varphi_i+\psi(t)\right)-\sin\varphi_i\right] \\
&\quad +\hat{r}(t)\dot{\psi}(t)\cos\left(\varphi_i+\psi(t)\right), \\
\dot{\alpha}_c(t) &= \dot{\psi}(t).
\end{aligned}$$

From (17) and (18) it can be easily shown that the simple proportional control law

$$\begin{aligned}
\dot{\hat{r}}(t) &= \lambda_r e_u(t), \\
\dot{\psi}(t) &= -\lambda_a e_s(t)
\end{aligned} \tag{20}$$

is such that (for suitable positive λ_r and λ_a)

$$\lim_{t\to\infty} c'(t) = c.$$

Fig. 7 shows the trajectories followed by the camera for four different initial estimates $\hat{r}_0$ of the unknown circular radius $r = 1$. Control parameters were set to $\lambda_r = 1$, $\lambda_a = 0.1$. Further details on the controller design can be found in [2].

Observe also that in this case visual servoing (20) is entirely defined in terms of image measurements. The estimation of the epipoles is given by the solution of an optimization problem similar to (11) which has two free parameters (the two x-coordinates of the epipoles) instead of one and is constrained by the tangency condition in each view.

4 General planar motion

In this section the case of general cameras displacement is discussed. No a priori knowledge of the rotation and translation between the initial and the final positions is given. Assume only that the optical axes of the camera-robot in the initial and final configurations intersect at a point o. This case is that of general cameras displacement depicted in Fig. 3, where the property of symmetry discussed in Remark 1 does not apply.

Consider the trajectory consisting of a translation along the optical axis and a rotation about the axis through o, leading the camera from the initial configuration to the final one.

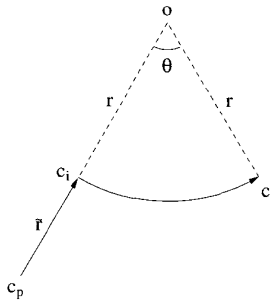

Figure 8: Trajectory followed by the robot in the case of general planar motion.

In order to reach the desired position, the visual servoing algorithm steers the robot along this trajectory in two steps:

1. the robot starts translating along the optical axis to reach a distance from o equal to r (i.e. to make $\tilde{r} = 0$ in Fig. 3);
2. the robot moves to the desired position with a circular motion.

Observe that the first step does not require knowledge of the current or desired radius. In fact it consists of a simple translation along the optical axis and the stopping condition occurs when parameter e_u (15), accounting for non-circular displacements, goes to zero. A simple proportional control law can be chosen as

$$\dot{\tilde{r}}(t) = \lambda e_u(t) \tag{21}$$

for some $\lambda > 0$ and, consequently, the robot differential kinematics become

$$\begin{aligned}
\dot{Z}_c(t) &= \lambda e_u(t) Z_c(t), \\
\dot{X}_c(t) &= \lambda e_u(t) X_c(t), \\
\dot{\alpha}_c(t) &= 0.
\end{aligned}$$

The second step brings the robot to the desired position following a circular trajectory as described in the previous section. Observe that neither knowledge nor estimation of the trajectory radius is required. Fig. 8 shows the complete trajectory followed by the camera in the case of general camera displacement from an initial configuration c_p to the final configuration c.

5 Simulations

Simulation results are reported to validate the proposed visual servoing algorithm for holonomic mobile robots.

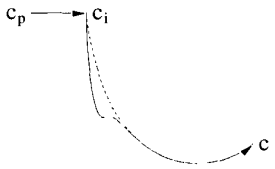

Figure 9: General planar motion: $\hat{r}_0 = 3r$ (solid) and $\hat{r}_0 = 0$ (dashed).

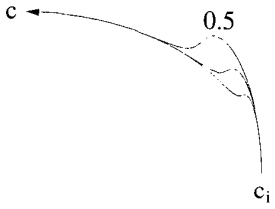

Figure 10: Trajectory for $\hat{r}_0 = 3r$ and different values of λ_r $(0.5, 1, 2)$.

General planar motion was tested. The initial and final robot-camera configurations are

$$\begin{pmatrix} Z_{c_i} \\ X_{c_i} \\ \alpha_{c_i} \end{pmatrix} = \begin{pmatrix} -0.866 \\ -0.5 \\ \pi/3 \end{pmatrix}; \quad \begin{pmatrix} Z_c \\ X_c \\ \alpha_c \end{pmatrix} = \begin{pmatrix} -0.866 \\ 0.5 \\ 2\pi/3 \end{pmatrix}.$$

Fig. 8 shows the ideal translational and rotational trajectories followed by the visual servoing. The pure translation moves the robot along the optical axis from c_p to the intersection c_i with the circle passing through c and centered on o. From this point the robot-camera starts to rotate as described in Section 3.2. This second part of the trajectory, which steers the mobile robot to c, strongly depends on the initial guess of the unknown radius r. Simulations are reported in Fig. 9: the solid line (dashed line) corresponds to an initial guess which is three (zero) times the true value. Control parameters are set to $\lambda = 1$, $\lambda_r = 1$ and $\lambda_a = 0.1$.

A second simulation was run to show system behavior for different control parameters. Circular motions with unknown radius were considered. Fig. 10 shows the trajectories followed for $\hat{r}_0 = 3r$, $\lambda_a = 1$ and different values of λ_r.

6 Conclusions

Epipolar geometry was exploited to design an image-based visual servoing algorithm for a mobile robot with a fixed camera. For the sake of simplicity mobile robot kinematics was assumed to be holonomic and the camera intrinsic parameters were assumed partially known. These assumptions can be relaxed to less restrictive conditions at the cost of a more involved discussion that, however, would not improve the problem insight.

The visual servoing algorithm is based on a measure of the symmetry of the epipolar geometry which is retrieved using image contours and tangency constraints but without solving any correspondence problem. Exploiting profiles in visual feedback is crucial in outdoor navigation where objects in the scene are highly unstructured and solving for correspondences is difficult.

Work is in progress to test the visual servoing algorithm on an experimental platform, the XR4000 by Nomadic Inc.

Acknowledgments

The authors wish to thank the student Massimo Pasqualetti of the University of Siena for his support in running simulations.

References

[1] G. Chesi, E. Malis, R. Cipolla: Automatic segmentation and matching of planar contours for visual servoing. In *Proc. Int. Conf. Rob. Autom.*, San Francisco, Cal., 2000.

[2] G. Chesi, D. Prattichizzo, A. Vicino. "Exploiting profiles in visual servoing", Int. Rep., Univ. of Siena, 2000.

[3] R. Cipolla and P.J. Giblin: *Visual Motion of Curves and Surfaces.* Cambridge University Press, 2000.

[4] F. Conticelli, D. Prattichizzo, A. Bicchi, F. Guidi, "Vision-Based Dynamic Estimation and Set-Point Stabilization of Nonholonomic Vehicles". In *Proc. Int. Conf. Rob. Autom.*, San Francisco, Cal., 2000.

[5] O. Faugeras: *Three-Dimensional Computer Vision: A Geometric Viewpoint.* MIT Press, Cambridge, 1993.

[6] K. Hashimoto and T. Noritsugu. "Visual servoing of nonholonomic cart". In *Proc. Int. Conf. Rob. Autom.*, Albuquerque, New Mexico, 1997.

[7] S. Hutchinson, G.D. Hager, and P.I Corke. "Tutorial on visual servo control". *IEEE Trans. Rob. Autom.*, 12(5):651–670, 1996.

[8] G.D. Hager, D.J. Kriegman, A.S. Georghiades, and O. Ben-Shahar. "Toward domain-independent navigation: dynamic vision and control". In *Proc. Conf. on Dec. and Control*, Tampa, Fl., 1998.

[9] P.R.S. Mendonca and R. Cipolla: Estimation of epipolar geometry from apparent contours: affine and circular motion cases. *Proc. IEEE Conf. Comp. Vis. Patt. Rec.*, Fort Collins, Col., I:9–14, 1999.

[10] P.R.S. Mendonca, K-Y.K. Wong and R. Cipolla: Circular motion recovery from image profiles. *Proc. of Workshop on Vision Algorithms: Theory and Practice*, Corfu, Greece, pages 119–126, 1999.